



Improvement of water management in a vapor feed direct methanol fuel cell

M. Shahbudin Masdar, Takuya Tsujiguchi, Nobuyoshi Nakagawa*

Department of Chemical and Environmental Engineering, Graduate School of Engineering, Gunma University, 1-5-1 Tenjin-cho, Kiryu, Gunma 376-8515, Japan

ARTICLE INFO

Article history:

Received 17 May 2010

Received in revised form 29 June 2010

Accepted 30 June 2010

Available online 7 July 2010

Keywords:

Water transport

Vapor feed DMFC

Porous carbon plate

Hydrophobic air filter

Mass spectrometry

ABSTRACT

Water transport in a vapor feed direct methanol fuel cell was improved by fixing a hydrophobic air filter (HAF) at the cathode. Effects of the HAF properties and the fixed positions, i.e., just on the cathode surface or by providing a certain space from the surface, of the HAF on the water transport as well as the power generation performance were investigated. The water transport was evaluated by measuring the partial pressure of water, P_{H_2O} , and methanol, P_{CH_3OH} , at the anode gas layer using in situ mass spectrometry with a capillary probe and also the water and methanol fluxes across the electrode structure using a conventional method. The HAF with the highest hydrophobicity and the highest flow resistance had the strongest effect on increasing the water back diffusion from the cathode to the anode through the membrane and increasing the current density. It was noted that the HAF fixation by providing a space from the cathode surface was more effective in increasing JWCO and the current density than that of the direct placement on the cathode surface. There was an optimum distance for the HAF placement depending on the humidity of the outside air.

© 2010 Elsevier B.V. All rights reserved.

1. Introduction

Direct methanol fuel cells (DMFCs) have received special attention as a portable power source for mobile electronic devices due to their low operating temperature and high power density [1–3]. One of the fundamental factors that prevent DMFCs from faster development is methanol crossover (MCO). As a result of the MCO, the low concentrations of methanol from 1–3 M [4–6] under active conditions and about 5 M [7–9] under passive conditions have generally shown a maximum power generation performance of the liquid feed DMFC operation. However, a low methanol concentration leads to a low energy density of the fuel cell system, which cannot meet the current requirement.

We have demonstrated that application of a porous carbon plate (PCP) to the anode could increase the optimum methanol concentration to 16 M or higher, even to 100% (24.7 M), and reducing the MCO [10–14]. The mechanism of using such a high concentration has been investigated and clarified which involves the mass transport restriction through the PCP and through the gas layer with CO_2 formed on the surface of the anode [10–12]. The vapor pressure of methanol, P_{CH_3OH} , and water, P_{H_2O} , at the anode surface was controlled by the PCP properties [15]. The function of the anode structure with the PCP can very effectively increase the energy density of the DMFC system [14]. In the DMFC with

the PCP, the water required for the cathode reaction and for the hydration of the membrane is supplied from the cathode to the anode by the water back diffusion through the membrane [11], and hence, flooding, that easily occurs in a liquid feed DMFC, at the cathode hardly occurs. However, the water supply to the anode was sometimes limited, especially when the current density was high and/or methanol vapor pressure at the anode was high, $P_{CH_3OH} > 10$ kPa [15], resulting in a decreased output power. When the electrolyte membrane is too dehydrated, the proton conductivity of the membrane significantly decreases thus leading to the poor performance of the DMFC [13]. A water management that enhances the water back diffusion is important in the DMFC with the PCP, especially for operation at high methanol concentrations.

So far, in order to improve the water management in the cell, extensive efforts have been made [16–19]. Most of the studies have been done for the liquid feed DMFC and focused on the addition of a hydrophobic agent such as polytetrafluoroethylene (PTFE) to the cathode diffusion layer or to the cathode microporous layer (MPL). In a liquid feed DMFC, the optimum hydrophobic level could reduce the water content and its gradient across the membrane, and hence reduce the flooding at the cathode. On the other hand, there are a few papers that focused on the water management for the vapor feed DMFC [20–22]. For the water transport, Shaffer and Wang developed a 1-D model to improve the water management for operation at a high methanol concentration by introducing an anode transport barrier, an MEA with a hydrophobic MPL at the anode and the cathode [20]. Recently, Abdelkareem and Nakagawa obtained the same results by putting an air filter on the cathode side, thus

* Corresponding author. Tel.: +81 277 30 1458; fax: +81 277 30 1457.

E-mail addresses: nobnaka@sannet.ne.jp, nakagawa@cee.gunma-u.ac.jp (N. Nakagawa).

Table 1
Properties of the hydrophobic air filter (HAF).

Hydrophobic air filter (HAF)	Preparation	Thickness (μm)	Porosity (–)	Mean pore size (μm)	Darcy constant, k (m^2)	Contact angle with water ($^\circ$)
FL1	50 wt% teflonized carbon paper (TGH-H-060)	250	0.776	20.4	$3.49\text{E}-13$	<100
FL2	Compressed sheet of un-woven fabric with carbon black and PTFE	110	0.617	3.79	$3.90\text{E}-14$	127
FL3	Compressed sheet of un-woven fabric with carbon black and PTFE	130	0.583	1.11	$7.40\text{E}-15$	154

the performance of the vapor feed DMFC increased compared to that without the air filter [21].

In this study, the effect of fixing a hydrophobic air filter (HAF) on the power generation and the water management in the vapor feed DMFC operated with a high concentration of methanol was investigated. Three different types of HAFs with different properties were used and the position of the fixed HAF, i.e., fixing the HAF directly on the cathode and fixing it within a certain distance from the cathode was studied for the purpose of increasing the water back diffusion from the cathode to the anode and to increase the power output.

2. Experimental

2.1. MEA preparation

The MEA, in which Pt and Pt–Ru black were used as the catalyst for the cathode and anode, respectively, was prepared and fabricated in the same manner as described in our previous reports [10,11]. The catalyst loading was $7\text{--}8\text{ mg cm}^{-2}$ in each electrode while Nafion 112 was used as the electrolyte membrane. The MEA was then fabricated by sandwiching the membrane between the anode and the cathode and hot pressing them at 408 K and 5 MPa for 3 min.

2.2. Hydrophobic membrane used as the air filter

Three types of hydrophobic porous membranes were prepared and used as the hydrophobic air filter (HAF). They are listed in Table 1 along with their properties. FL1 was a teflonized (50 wt% PTFE) carbon paper (TGP-H-060, Toray). FL2 and FL3 were compressed non-woven fabrics with carbon black and PTFE. The thickness of the filters, contact angle with water on their surfaces and other properties related to their pore structures are shown in Table 1. FL3 had the highest hydrophobicity and the highest resistivity to fluid flow, i.e., lowest Darcy constant, among the three filters.

2.3. Setup for the DMFC with fixing HAF directly on the cathode

Fig. 1 shows the cell configuration and the experimental setup used for directly fixing the HAF on the cathode. The vapor feed DMFC was constructed with a methanol reservoir at the bottom, which supplies methanol vapor through the anode gas layer from the solution surface to the anode that was below of the electrolyte membrane. The top of the MEA was the cathode that contacted the air supplied by the micropump. In this configuration, the partial pressures of the methanol, $P_{\text{CH}_3\text{OH}}$, and water, $P_{\text{H}_2\text{O}}$, in the anode gas layer can be controlled by the methanol concentration and the level of the methanol solution in the reservoir, i.e., the distance between the solution level and the anode surface. The distance was maintained at 5.5 mm in this experiment including 0.5 mm for the microprobe spacer and 1.0 mm for the anode current collector. In

order to keep the distance, along the whole anode surface, constant, the cell was put in horizontally. The anode gas was analyzed using a mass spectrometer (MS) with a $30\text{ }\mu\text{m}$ inner diameter capillary probe [15]. The capillary probe was inserted through a hole in the spacer and placed at about 1.0 mm below from the anode surface.

The vapor feed DMFC was operated under ambient room conditions by injecting a methanol solution with a certain concentration into the reservoir and by feeding ambient air to the cathode at 300 ml min^{-1} . Such a high flow-rate for air was chosen to prevent the water produced at the cathode from accumulating in the cathode chamber and to accurately collect the water exhausted at the cathode in a cold trap. The power generation was conducted at the constant cell voltage of 0.2 V for 5 h. The electrochemical performance of the cell was measured using an HZ3000 electrochemical measurement system (Hokuto Co., Ltd.). The cell temperature was measured at the surface of the cathode by a thermocouple. Moreover, the ohmic cell resistance was measured during the cell operation using the AC m-ohm tester (TSURUGA Electric Corp.) with measuring frequency at 10 kHz.

2.4. Setup for the DMFC with HAF by leaving a space from the cathode

Fig. 2 shows the cell configuration and the experimental setup used for the HAF with a spacing from the cathode surface. The cell was placed upside down, opposite to the case in Fig. 1. The cathode was on the bottom and the anode was on the top of the MEA in this case. A porous carbon plate (PCP) with a certain property was placed between the anode current corrector and the methanol solution as shown in the figure. In this cell configuration, it has been confirmed, as in our previous papers [10–12,15], that an anode gas layer formed on the anode surface, i.e., in the pores of the anode current corrector and the PCP, and the electrode structure controls the MCO and $P_{\text{CH}_3\text{OH}}$ of the anode gas layer. The electrode structure with PCP enables the utilization of a high concentration, even 100% (24.7 M), of methanol fed to the reservoir of the DMFC [10–14].

The PCP used in this experiment was PCP-A, having a high resistivity to the methanol transport with a 15% porosity and a 0.5 mm thickness, and PCP-B, having a low resistivity with a 35% porosity and a 1.5 mm thickness.

At the cathode, HAF was fixed on the cathode current corrector with a 74% open ratio, and hence, a certain spacing, D , corresponding to the thickness of the current corrector between the HAF and the cathode surface as shown in Fig. 2. The distance was then varied from 1.5 to 10.0 mm by changing the thickness of the current corrector.

The DMFC and the microair pump were placed in an oven-chamber where the temperature and the humidity were controlled, and hence, the temperature and relative humidity (RH) of the air fed to the cathode was controlled at 303 K and RH values 30%, 60% and 90%.

The power generation was conducted at a constant cell voltage of 0.2 V for 6 h using the same equipment (HZ3000, Hokuto Co.,

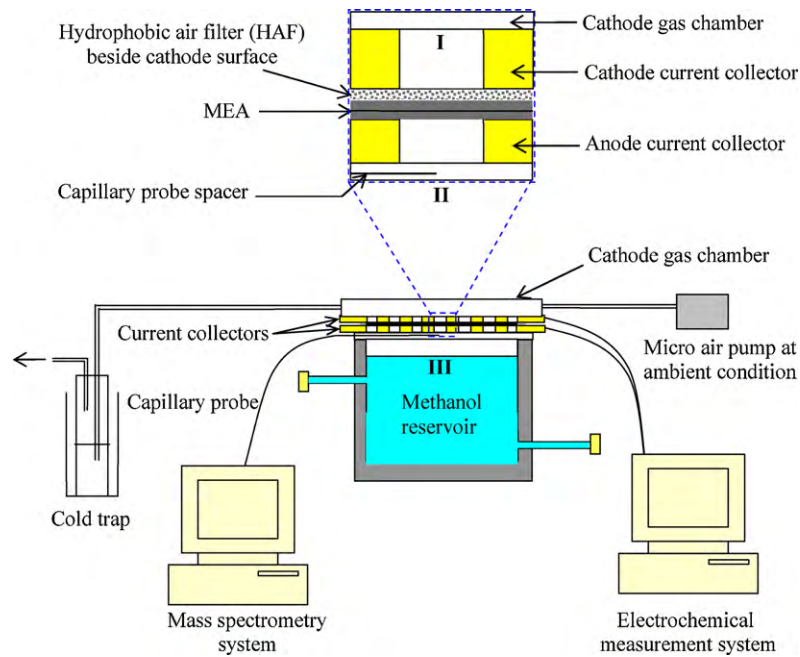


Fig. 1. Experimental setup for the vapor feed DMFC with HAF fixed directly on the cathode surface.

Ltd.) as well as the cell temperature and the cell resistance were measured and procedures as that in Fig. 1.

2.5. Water, methanol crossover evaluation and MS analysis

The average water crossover (WCO), J_{WCO} , and average methanol crossover (MCO), J_{MCO} , through the MEA during the cell operation were evaluated on the basis of the losses of methanol and water in the reservoir subtracted by the amounts that used for the anode reaction assuming the complete oxidation of methanol to CO_2 . To do this, a weight loss of the solution in the reservoir was measured, and concentrations of methanol and water in the solution were analyzed before and after the cell operation using a gas chromatography. Then, the charge passed also was calculated by

integrating the area of the $i-t$ curve. The procedure of evaluation of the fluxes was described in detail in our previous paper [11]. For the mass spectral analyses of the water and other components in the gas layer, a quadrupole mass spectrometer (DME 100 MS, Ametek Process Instruments) with a capillary probe was used during the cell operation. The detailed procedure of these measurements and the evaluation methods were similar to that described in our previous report [15].

2.6. Calculation of the water balance in the cell

For the water balance consideration in the cell, Fig. 3 shows a schematic of the water transport in the cell. In the DMFC, the water produced at the cathode was the sum of that produced by

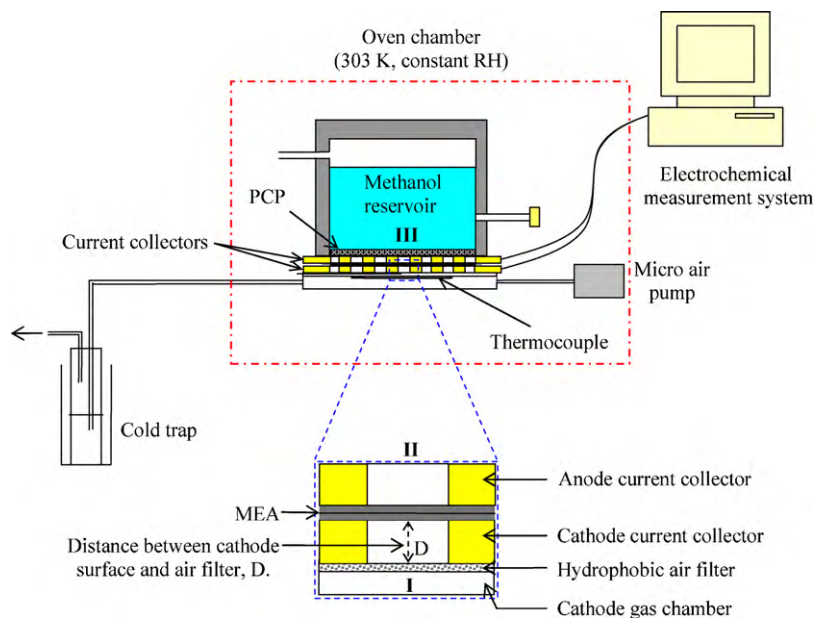


Fig. 2. Experimental setup for the vapor feed DMFC with HAF fixed at a specific distance from the cathode surface in the chamber with a controlled temperature and air humidity.

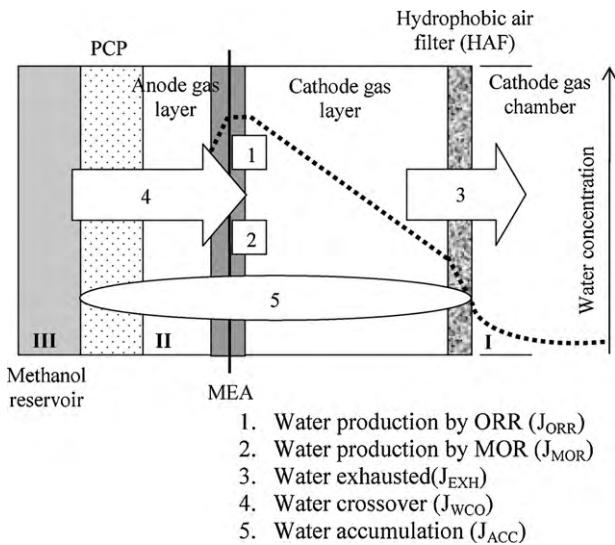
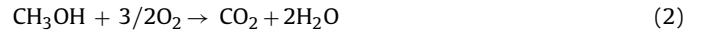


Fig. 3. Schematic of water transport in the vapor feed DMFC with PCP and HAF at a specific distance D .

the oxygen reduction reaction (ORR), J_{ORR} , and that by the oxidation of the methanol crossover, J_{MOR} , as described in Eqs. (1) and (2), respectively.



Hence, the water flux by the ORR, J_{ORR} , can be calculated as follows:

$$J_{ORR} = iM_{H_2O}/(2F) \quad (3)$$

where i is the current density, M_{H_2O} is the molar mass of water and F is the Faraday constant. The methanol transported to the cathode by the MCO was assumed to be completely oxidized to CO_2 at the cathode, and then the water flux, J_{MOR} , can be expressed as

$$J_{MOR} = 2J_{MCO} \quad (4)$$

Therefore, the following relationship describes the water transport in the cell.

$$J_{ORR} + J_{MOR} + J_{WCO} = J_{ACC} + J_{EXH} \quad (5)$$

where J_{EXH} is the flux of water exhausted from the cathode outlet, while J_{ACC} is the water accumulation in the cell structure during the measurement.

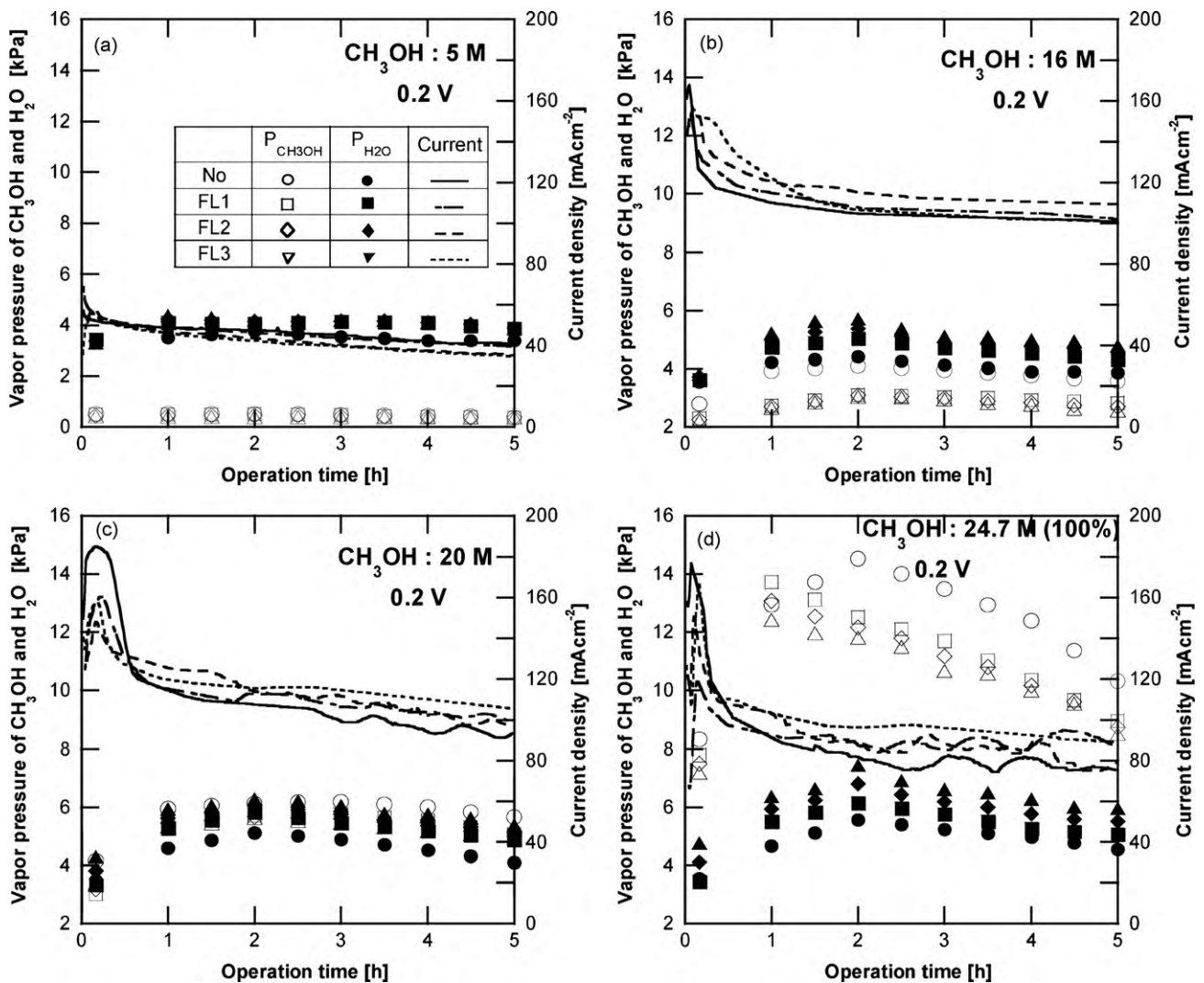


Fig. 4. Profiles of current density, P_{CH_3OH} and P_{H_2O} with time for the vapor feed DMFC with different HAFs fixed directly on the cathode surface and those without it; (a) 5 M, (b) 16 M, (c) 20 M, (d) 24.7 M (100%).

3. Results and discussion

3.1. Effect of directly fixing HAF on the cathode

Fig. 4(a–d) shows the profile of the current density, vapor pressure of methanol, $P_{\text{CH}_3\text{OH}}$, and water, $P_{\text{H}_2\text{O}}$, versus the operation time with the different hydrophobic air filter (HAF) directly fixed on the cathode surface and those without it. Each figure was prepared for the specific methanol concentration in the reservoir.

For all the cases, (a–d), in this figure, at the beginning of cell the operation, the current densities were unstable with time, they sharply increased and then decreased before they became stable. The unstable current density would be related to the initial methanol that accumulated in the anode under the open circuit conditions as has been explained in our previous reports [11,13]. $P_{\text{CH}_3\text{OH}}$ and $P_{\text{H}_2\text{O}}$ depend on the methanol concentration in the reservoir, and those increased with the increasing methanol concentration. The initial increase in $P_{\text{H}_2\text{O}}$ would be due to the time delay of the backwater diffusion from the cathode to the anode, while the decreasing $P_{\text{CH}_3\text{OH}}$ with time would be related to the high consumption of methanol at the anode based on the high current densities. These profiles of $P_{\text{CH}_3\text{OH}}$ and $P_{\text{H}_2\text{O}}$ have been described in detail in our previous paper [15].

It was clear from the figure that $P_{\text{H}_2\text{O}}$ and $P_{\text{CH}_3\text{OH}}$ in the anode gas layer increased and decreased, respectively, by directly fixing the HAF on the cathode resulting in an increase in the current density. At the low $P_{\text{CH}_3\text{OH}}$ below 1 kPa, Fig. 4(a), this effect was quite small and was not clear. However, it became clear with the increasing $P_{\text{CH}_3\text{OH}}$ in the anode gas layer. At the high $P_{\text{CH}_3\text{OH}}$ over 8 kPa, Fig. 4(d), those increases or decreases induced by fixing the HAF were significant, and the magnitude of the increase or decrease depended on the HAF being used. The magnitude of the increasing current density and the increasing $P_{\text{H}_2\text{O}}$ was observed to display the following trend in decreasing current density: FL3 > FL2 > FL1. For instance, it appears to be approximately a 15%, 12% and 6% increase in current density for FL3, FL2 and FL1, respectively, compared without HAF when using 20 M methanol concentration in the reservoir as shown in Fig. 4(c). This order was agreed with that of the resistivity for the fluid flow, i.e., the inverse of the Darcy's constant, and also that of the hydrophobicity, i.e., the contact angle, as shown in Table 1. It was then concluded that the stronger the resistivity and the hydrophobicity of the HAF, the higher $P_{\text{H}_2\text{O}}$ in the anode gas layer and the higher current density.

The higher $P_{\text{H}_2\text{O}}$ in the anode gas layer suggested a higher water flux from the cathode to the anode. Fig. 5 shows the relationship between the steady current density measured at 3 h from the start and the water crossover, J_{WCO} , at various $P_{\text{CH}_3\text{OH}}$ values during a 3 h operation shown in Fig. 4(a–d) including some additional data at 8 M and 12 M methanol concentrations in the reservoir. For all the cases with the different HAFs or without it, the current density linearly increased up to a certain $P_{\text{CH}_3\text{OH}}$, around 3 kPa, along with the common straight line in the figure suggesting that the current densities in this region, $P_{\text{CH}_3\text{OH}} < 3$ kPa, were controlled by the methanol supply rate to the anode. This was very clear from the linear dependency of the current density on $P_{\text{CH}_3\text{OH}}$. In the high $P_{\text{CH}_3\text{OH}}$ region, $P_{\text{CH}_3\text{OH}} > 3$ kPa, the current density decreased from the maximum current density depending on the type of HAF. The magnitude of the current density in this region was high in the order of FL3, FL2, FL1 and then no HAF.

The J_{WCO} was also plotted versus $P_{\text{CH}_3\text{OH}}$ in the figure using the open symbols with the vertical axis on the right hand side. The negative value of J_{WCO} means the direction of the transport was from the cathode to the anode. For all cases, J_{WCO} negatively increased with the increasing $P_{\text{CH}_3\text{OH}}$. The J_{WCO} significantly decreased, negatively increased, in the range of the low $P_{\text{CH}_3\text{OH}}$, i.e., $P_{\text{CH}_3\text{OH}} < 3$ kPa, and then slightly decreased in the range of $P_{\text{CH}_3\text{OH}} > 3$ kPa

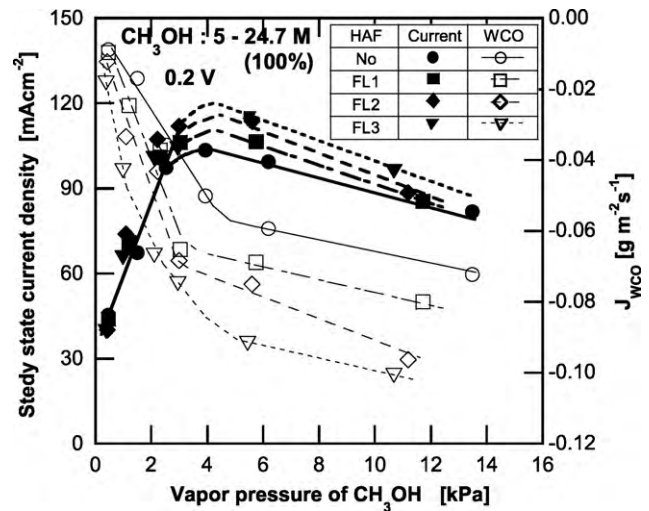


Fig. 5. The steady current density and the average water crossover, J_{WCO} , at various $P_{\text{CH}_3\text{OH}}$ for the DMFC with different HAFs fixed directly on the cathode surface.

depending on the type of HAF. When J_{WCO} at a certain $P_{\text{CH}_3\text{OH}}$ was compared among the three filters used, one can understand that the higher hydrophobicity of the filter, the more negative J_{WCO} . The highest current density was obtained by FL3 due to the negative increase in the water flux in the range of the high $P_{\text{CH}_3\text{OH}}$.

When the cell was operated at a high $P_{\text{CH}_3\text{OH}} > 3$ kPa, the region that is out of the methanol transport limitation, the current density decreased with the increasing $P_{\text{CH}_3\text{OH}}$. In this region, either the electrode reactions or the water supply to the anode, or both of them, would control the current density.

Someone may consider that the increase in the current density with HAF was smaller than that expected from the decrease in J_{WCO} which was sometimes nearly 40% more negative compared to that without the HAF. One of the reasons can be explained by the higher cell resistance for the HAF due to the high cell resistance, 10–35% higher compared to that without the HAF, of HAF itself including its contact resistance. Hence, fixing the HAF directly on the cathode may not be effectively improve the vapor feed DMFC performance, although the water flux was significantly improved. In the next section, the position of the HAF was changed by leaving a space from the cathode surface.

3.2. Effect of fixing HAF by leaving a space from the cathode

3.2.1. Comparison of the cases with and without HAF at different air humidities

Fig. 6 shows the profiles of the current density for the cases with and without the HAF (FL3) that was fixed with placing it 2.5 mm from the cathode surface at different air humidities using the setup shown in Fig. 2. In this measurement, the methanol solution was replaced with that of a fresh one after the first 3 h of operation in order to avoid any error in the evaluation of the water and methanol fluxes that were calculated as an average value during the measurement, because we sometimes observed a large variation in the current density in the first 3 h of operation as shown in the figure. The large variation in the current density would be caused by the initial condition, which was different from the steady state under the specified operating conditions of the atmosphere at the electrode. The evaluation was conducted for the next 3 h of operation after replacement of the solution.

As is clear from Fig. 6, the effect of the air humidity on the steady current density was significantly high for the cases without the HAF. This was mainly caused by the dehydration of the electrolyte membrane that clearly reflected an increase in the cell resistance

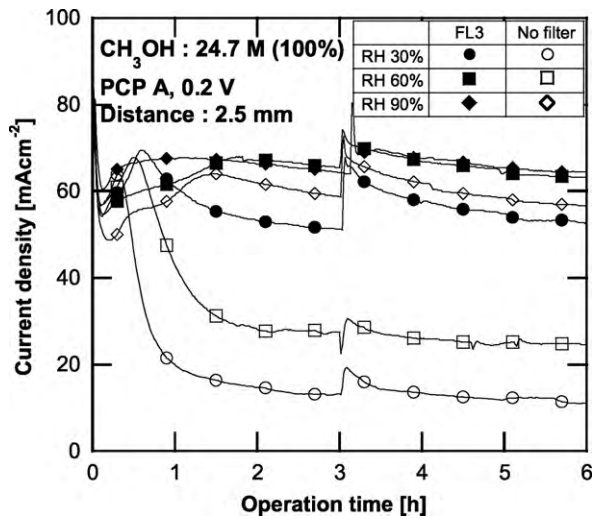


Fig. 6. Current density profiles at different air humidities, RH, for the cases with and without HAF (FL3) fixed at a distance of 2.5 mm.

with a decrease in the relative humidity (RH) as shown in Table 2. It was clear that a high relative humidity like an RH 90% in the air was necessary to keep the current density high for no HAF at the cathode. On the other hand, the current density reduced by the dehydration was significantly improved by fixing the HAF (FL3) with a space 2.5 mm from the cathode surface. The reduced current density of 12 mA cm^{-2} for RH 30% was improved up to 53 mA cm^{-2} that was almost 95% of that at RH 90% by the fixing of FL3. The water flux, J_{WCO} , and the methanol flux, J_{MCO} , in the experiments shown in Fig. 6 are also summarized in Table 2. From the table, it was clear that for all the cases with different humidities, J_{WCO} was negatively increased while J_{MCO} and the cell resistance decreased by fixing the HAF, i.e., FL3, compared to that without it. It can be confirmed that the fixation of HAF (FL3) with a certain space improved the water management by reducing the water exhausted, J_{EXH} , and then negatively increased the water flux, J_{WCO} , of the DMFC. HAF at the cathode would be necessary, especially when the cell was operated at a low air humidity.

3.2.2. Comparison of directly fixing HAF on the cathode and that with a space from the cathode

To clarify the difference between the HAF fixation directly on the cathode surface and HAF fixation at a certain distance, an experiment was conducted using the setup shown in Fig. 2. Using PCP-B and a methanol solution of 16 M, the cell was operated for different two cases, i.e., by fixing FL3 between the cathode and the cathode current collector; i.e., direct contact, and by fixing FL3 on the outer surface of the current collector (1.5 mm thick); i.e., with a 1.5 mm space from the cathode. Table 3 shows a comparison of the steady current density, cell resistance, water fluxes and J_{MCO} for the different two cases.

Table 2

Cell resistance, water transport and J_{MCO} for the operation with and without the HAF (FL3) by leaving a 2.5 mm space at different air humidities.

	RH 30%		RH 60%		RH 90%	
	FL3	No filter	FL3	No filter	FL3	No filter
Cell resistance ($\text{m}\Omega$)	65.80	245.1	44.30	155.8	35.80	71.80
$J_{\text{ORR+MOR}}$ ($\text{g m}^{-2} \text{ s}^{-1}$)	0.078	0.062	0.069	0.057	0.079	0.088
J_{EXH} ($\text{g m}^{-2} \text{ s}^{-1}$)	0.020	0.063	0.012	0.0630	0.008	0.010
J_{ACC} ($\text{g m}^{-2} \text{ s}^{-1}$)	0.037	0.002	0.029	0.016	0.034	0.049
J_{WCO} ($\text{g m}^{-2} \text{ s}^{-1}$)	-0.021	-0.003	-0.029	-0.012	-0.037	-0.029
J_{MCO} ($\text{g m}^{-2} \text{ s}^{-1}$)	0.077	0.170	0.032	0.132	0.016	0.030

Table 3

Stable current density, cell resistance, water transport and J_{MCO} for the operation using an HAF directly fixed on the cathode surface and by providing a 1.5 mm space at RH 60%.

	Distance 1.5 mm	Direct contact
Stable current density at 0.2 V (mA cm^{-2})	105.4	92.14
Cell resistance ($\text{m}\Omega$)	50.47	55.32
$J_{\text{ORR+MOR}}$ ($\text{g m}^{-2} \text{ s}^{-1}$)	0.184	0.176
J_{EXH} ($\text{g m}^{-2} \text{ s}^{-1}$)	0.110	0.131
J_{ACC} ($\text{g m}^{-2} \text{ s}^{-1}$)	0.007	0.001
J_{WCO} ($\text{g m}^{-2} \text{ s}^{-1}$)	-0.059	-0.045
J_{MCO} ($\text{g m}^{-2} \text{ s}^{-1}$)	0.076	0.082

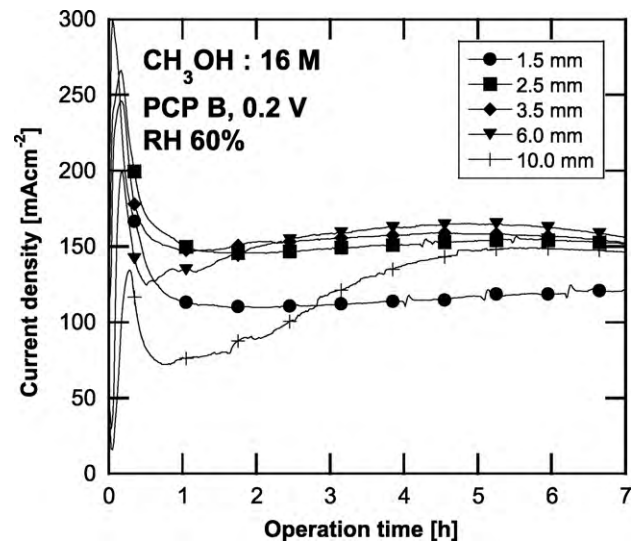


Fig. 7. Current density profiles for the cases with HAF (FL3) with leaving different distance at RH 60%.

From Table 3, it was clarified that the current density for the 1.5 mm distance was higher than that for the direct contact. This was mainly due to the water management at the 1.5 mm distance showing a high negative water crossover, J_{WCO} . Although the higher current density for the 1.5 mm distance was partly a result from the lower cell resistance that did not contain the resistance of FL3, the reduced J_{EXH} for the 1.5 mm distance should be noted. By leaving a distance between the HAF (FL3) and the cathode surface, the water flux exhausted to the outside decreased and then the water back diffusion was enhanced which resulted in the higher current density. The fixation of HAF by leaving a certain space was better than that directly on the cathode surface.

3.2.3. Effect of space D between the HAF and cathode surface

Fig. 7 shows the profiles of the current density of the DMFC with the HAF, FL3, fixed with a different space D , from $D = 1.5$ – 10.0 mm, from the cathode surface measured by the setup shown in Fig. 2. PCP-B and the 16 M methanol solution were used in the cell and the DMFC was operated at 0.2 V and RH 60%.

One can see that the profiles of the current density were dependent on the distance D . For example, the time required for the current to become stable increased with the increasing distance. When $D=1.5$ mm, the current density became constant after 1 h, while it required about 5 h when $D=10.0$ mm. Moreover, the stable current density increased with the increased distance from $D=1.5$ – 6.0 mm, then decreased at $D=10.0$ mm. The different distances mean the different mass transport resistances in the cathode gas layer.

To clarify the effect of the distance, D , on the cell performance, the stable current densities at 5 h in the measurements of Fig. 7 were plotted in Fig. 8 including additional data obtained at RH values of 30% and 90% with the cell resistance and J_{MCO} during operation. In all the cases at RH values of 30%, 60% and 90%, a similar trend in that the current density increased with the increasing distance up to a certain distance, that was dependent on RH, and then decreased with the increasing D . For RH 60%, the maximum current density of 165 mA cm^{-2} was obtained at $D=6.0$ mm, while for RH 90%, it was 154 mA cm^{-2} at $D=2.5$ mm. A large space $D > 6.0$ mm was required for the RH 30% in order to reach the maximum current.

One of the reasons for the increase in the current density with D was due to the decrease in the cell resistance as shown in Fig. 8. As it has already been discussed in Fig. 6 and Table 2, the fixation of HAF negatively increased the water crossover, J_{WCO} , by reducing the water exhausted, J_{EXH} , and it reduced the cell resistance

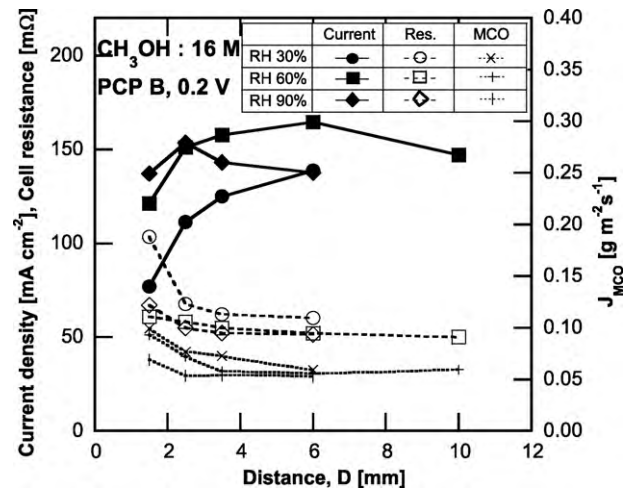


Fig. 8. Current density, cell resistance and J_{MCO} for the cases with HAF (FL3) at different distances and different air humidities.

and increased the current density. It was clear that the space D is another parameter that affects the water management in the cell.

Fig. 9 shows the water transport characteristics, i.e., the water produced by the oxygen reduction reaction (ORR) and methanol

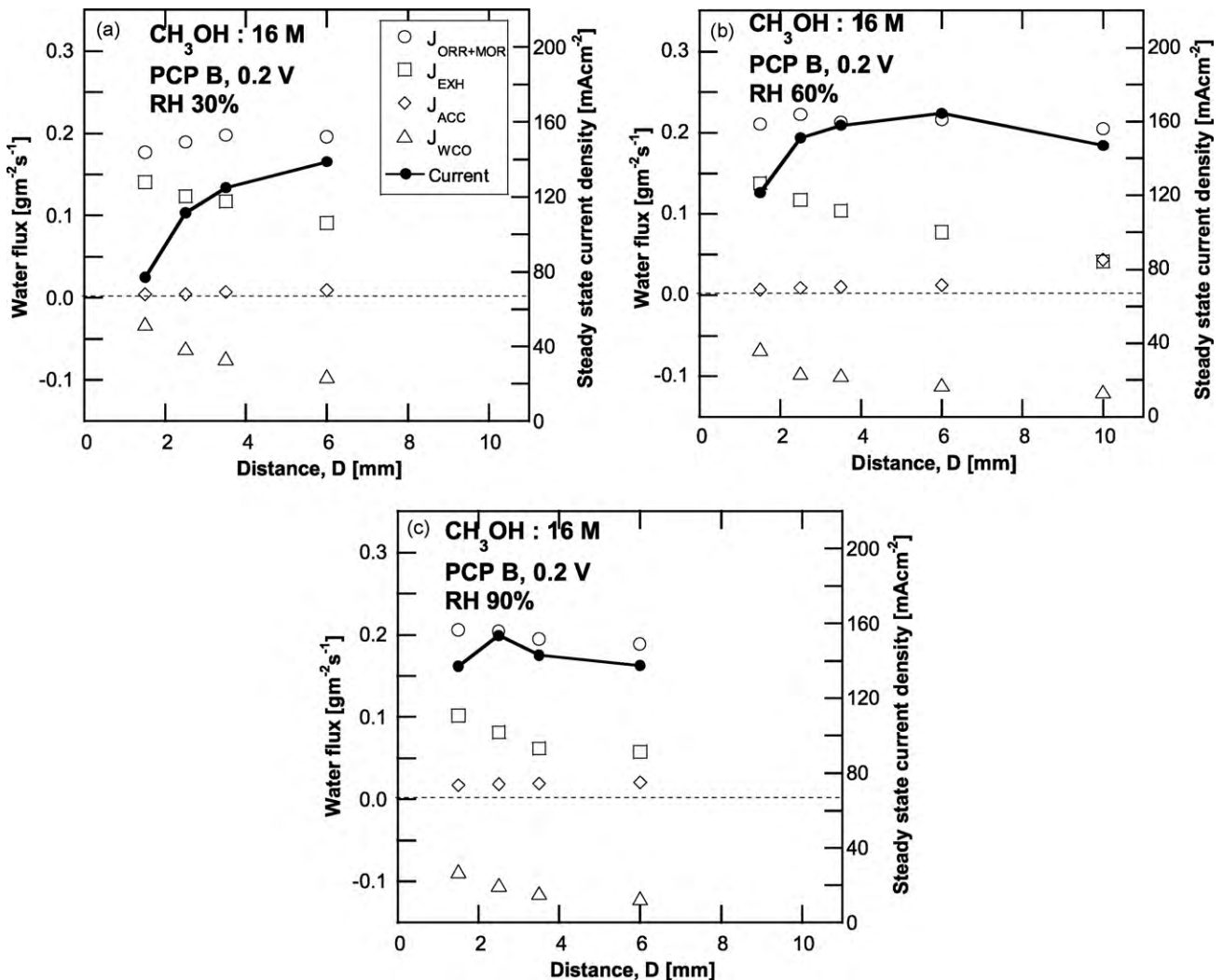


Fig. 9. Water transport at different D and air humidity values, (a) RH 30%, (b) RH 60%, (c) RH 90%.

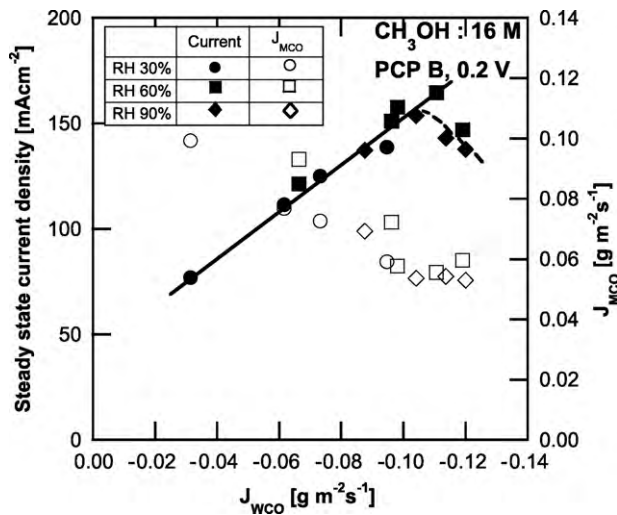


Fig. 10. Relationships among J_{MCO} and the current density as well as J_{WCO} for the HAF (FL3) with different spaces at different air humidities.

oxidation reaction (MOR), $J_{ORR+MOR}$ ($J_{ORR} + J_{MOR}$), water exhausted, J_{EXH} , water accumulated in the cell, J_{ACC} , at different D values for the experiments with different air humidities, RH 30%; (a), 60%; (b), and 90%; (c). For all the cases with the different air humidities, the water exhausted, J_{EXH} , decreased with the increasing distance by keeping the water production, $J_{ORR+MOR}$, almost constant. The mechanism for the decrease in J_{EXH} with D could be explained by the decrease in the transport rate of the water vapor through the cathode gas layer and HAF with the increasing distance according to Fick's first law. The decrease in J_{EXH} with D resulted in the negative increase in J_{WCO} and then the current increased with D . However, for too high a space, over the optimum distance, the current density decreased. In this condition, water accumulation, J_{ACC} , occurred and then J_{WCO} did not further negative decrease. J_{ACC} at nearly zero indicated that the water balance was achieved and the water transport in the cell was under steady state conditions.

When the air humidity was low, RH 30%, J_{EXH} at a certain distance was high compared to that RH values of 60% and 90%, because the driving force of the water transport through the gas layer and HAF, i.e., difference in the water vapor pressure between the cathode surface and the outside air, becomes high, according to the same mechanism of the water transport in the gas layer as mentioned above.

Fig. 10 shows the relationships between J_{WCO} and the current density for all the cases with different D values and different air humidities. In the figure, it was clearly shown that the current density linearly increased with the negative increasing J_{WCO} . The plots at too high a J_{WCO} over $-0.11 \text{ g m}^{-2} \text{ s}^{-1}$, where the water accumulation occurred, were off this line. The linear dependency means that the current densities were controlled by the water flux from the cathode to the anode, J_{WCO} . Meanwhile, the methanol crossover (MCO), J_{MCO} , decreased with the increasing of J_{WCO} . As the current density increased, the consumption of water and methanol

occurred at the anode according to the anode reaction, and then such a reciprocal relation between J_{WCO} and J_{MCO} would be shown.

The optimum design of the cathode structure with HAF for a specific space was quite important to increase the water back diffusion that was really required to prevent the deficiency in water at the anode, and the power output in the vapor feed DMFC that used methanol at high concentrations, even 100% (24.7 M).

4. Conclusion

The water management in the vapor feed direct methanol fuel cell was improved by fixing the hydrophobic air filter (HAF) to the cathode. The water exhausted to the cathode outside was reduced and then the water crossover, J_{WCO} , negatively increased by the HAF. It was confirmed, using in situ mass spectrometry, that the partial pressure of water, P_{H_2O} , increased by the HAF due to negative increase in J_{WCO} , and then resulting in an increase in the current density. This prevented the membrane from the dehydration that is related to the cell resistance. For the position of the HAF at the cathode, fixing the HAF with a proper distance was better than fixing it directly on the cathode surface, and there was an optimum distance depending on the outside air humidity. As HAF, FL3, which had the highest flow resistance and hydrophobicity, was the best to increase the current density when directly fixed on the cathode surface.

Acknowledgements

A part of this study was supported by KAKENHI (1936057).

References

- [1] C.Y. Chen, P. Yang, J. Power Sources 123 (2003) 37–42.
- [2] C. Xie, J. Bostaph, J. Pavio, J. Power Sources 136 (2004) 55–65.
- [3] H. Dohle, H. Schmitz, T. Bewer, J. Mergel, D. Stolten, J. Power Sources 106 (2002) 313–322.
- [4] S. Surampudi, S.R. Narayanan, E. Vamos, H. Frank, G. Halpert, A.L. Conti, J. Kosek, G.K.S. Prakash, G.A. Olah, J. Power Sources 47 (1994) 377–385.
- [5] M.K. Ravikumar, A.K. Shukla, J. Electrochem. Soc. 143 (1996) 2601–2606.
- [6] J. Ge, H. Liu, J. Power Sources 142 (2005) 56–69.
- [7] S.R. Yoon, G.H. Hwang, W.I. Cho, I.H. Oh, S.A. Hong, H.Y. Ha, J. Power Sources 106 (2002) 215–223.
- [8] R. Chen, T.S. Zhao, J. Power Sources 152 (2005) 122–130.
- [9] B. Bae, B.K. Kho, T. Lim, I.H. Oh, S.A. Hong, H.Y. Ha, J. Power Sources 158 (2006) 1256–1261.
- [10] N. Nakagawa, M.A. Abdelkareem, K. Sekimoto, J. Power Sources 160 (2006) 105–115.
- [11] M.A. Abdelkareem, N. Nakagawa, J. Power Sources 162 (2006) 114–123.
- [12] N. Nakagawa, M.A. Abdelkareem, J. Chem. Eng. Jpn. 40 (2007) 1199–1204.
- [13] M.A. Abdelkareem, N. Nakagawa, J. Power Sources 165 (2007) 685–691.
- [14] M.A. Abdelkareem, N. Morohashi, N. Nakagawa, J. Power Sources 172 (2007) 659–665.
- [15] M.S. Masdar, T. Tsujiguchi, N. Nakagawa, J. Power Sources 194 (2009) 610–617.
- [16] A. Blum, T. Duvdevani, M. Philosoph, N. Rudoy, E. Peled, J. Power Sources 117 (2003) 22–25.
- [17] G.Q. Lu, F.Q. Liu, C.Y. Wang, Electrochem. Solid-State Lett. 8 (2005) 1–4.
- [18] A. Oedegaard, C. Hebling, A. Schmitz, S.M. Holst, R. Tunold, J. Power Sources 127 (2004) 187–196.
- [19] C. Xu, T.S. Zhao, J. Power Sources 168 (2007) 143–153.
- [20] C.E. Shaffer, C.Y. Wang, J. Power Sources 195 (2010) 4185–4195.
- [21] M.A. Abdelkareem, N. Nakagawa, J. Key Eng. Mater., in press.
- [22] S. Eccarius, F. Krause, K. Beard, C. Agert, J. Power Sources 182 (2008) 565–579.